

The one-loop tadpole in the geoSMEFT

T. Corbett¹,

¹ Niels Bohr International Academy,
Niels Bohr Institute, University of Copenhagen,
Blegdamsvej 17, DK-2100, Copenhagen, Denmark
* corbett.t.s@gmail.com

September 12, 2021

1 Abstract

Making use of the geometric formulation of the Standard Model Effective Field Theory we calculate the one-loop tadpole diagrams to all orders in the Standard Model Effective Field Theory power counting. This work represents the first calculation of a one-loop amplitude beyond leading order in the Standard Model Effective Field Theory, and discusses the potential to extend this methodology to perform similar calculations of observables in the near future.

8

9 Contents

10	1 Introduction	1
11	2 Conventions	3
12	3 The all-orders vertices	7
13	4 Gauge fixing the geoSMEFT	9
14	5 The all-orders SMEFT tadpole	11
15	6 Conclusions	14
16	A Useful geoSMEFT definitions and relations	16
17	B Relevance of the tadpole to renormalization	17
18	References	18

19

20

21 1 Introduction

The Standard Model Effective Field Theory (SMEFT) has become a cornerstone of LHC searches for physics beyond the Standard Model (SM). The approach of the SMEFT is to search for the effects of non-resonant heavy new physics, which decouples as $1/\Lambda$, on measurable processes of the known particles. This approach makes two primary assumptions,

26 that the new physics is too heavy to directly produce at a collider and that the Higgs
 27 boson belongs to an $SU(2)_L$ doublet, as in the SM. With these assumptions the SMEFT
 28 is formulated as a tower of higher-dimensional operators suppressed by the new physics
 29 scale Λ and added to the SM Lagrangian:

$$\mathcal{L}_{\text{SMEFT}} = \mathcal{L}_{\text{SM}} + \sum_{n=5}^{\infty} \sum_i \frac{c_i}{\Lambda^{n-4}} \mathcal{O}_i. \quad (1)$$

30 Each subsequent power of $1/\Lambda$ should therefore be suppressed relative to the last, as Λ is
 31 a large mass scale well above that of a given scattering process.

32 For most LHC relevant processes the leading terms come from dimension-six operators
 33 suppressed by Λ^2 . There is ongoing discussion on how to handle the truncation of this
 34 series in the literature, i.e. to understand the error associated with truncating the series
 35 at a given order. Many groups have included squares of dimension-six operator contribu-
 36 tions to amplitudes in their work, this allows for an inferred error by comparing results
 37 with and without the dimension-six squared term. This presents a theoretical concern –
 38 formally this is not the full contribution at order $1/\Lambda^4$ as it neglects dimension-six squared
 39 contributions to the amplitude as well as dimension-eight operator effects. There is also
 40 the more practical issue, that in many instances the squared term results in more stringent
 41 constraints, a result of, for example, chiral suppression of the interference of the $1/\Lambda^2$ term
 42 with the SM. This makes a definition of truncation error in this way less than satisfactory.

43 An alternative approach is to compute the full contribution up to and including $\frac{1}{\Lambda^4}$
 44 effects. This suffers from the seemingly insurmountable number of parameters in the
 45 SMEFT beyond leading order. This is to a great degree controlled by only considering
 46 resonant processes where four-fermion operators can be neglected as well as making sim-
 47 plifying assumptions on the flavor structure of the SMEFT. To date three works have
 48 considered the full $\frac{1}{\Lambda^4}$ dependence in phenomenological studies. In [1], the authors study
 49 associated production of a Higgs boson with a W by meticulously elaborating all operators
 50 contributing via the Hilbert series method [2–4], and then performing a phenomenological
 51 study. Using a similar procedure the authors of [5] study the Drell Yan process at the
 52 LHC. In [6], the authors studied Z -pole observables and instead used the geometric for-
 53 mulation of the SMEFT which allows for, currently in limited cases, all orders calculations
 54 in the SMEFT power counting (i.e. the $1/\Lambda$ power counting).

55 The geometric SMEFT, or geoSMEFT, was born of an attempt to simplify the one loop
 56 calculation of $H \rightarrow \gamma\gamma$ [7, 8] and the resulting background gauge fixing of the SMEFT [9].
 57 Within this context it was realized that the SMEFT could be formulated in terms of
 58 *field-space connection matrices* of the form:

$$M_{I_1 \dots I_n} \sim \frac{\delta^n \mathcal{L}_{\text{SMEFT}}}{\delta\phi_{I_1} \dots \delta\phi_{I_n}} \Big|_{\mathcal{L}(\alpha, \beta, \dots) \rightarrow 0}. \quad (2)$$

59 These field-space connections are then matrices of products of the Higgs doublet with
 60 generators of $SU(2)_L$, and the evaluation at $\mathcal{L}(\alpha, \beta, \dots) \rightarrow 0$ represents setting various
 61 products of fields and their derivatives to zero. By constructing all gauge-variant, but
 62 Lorentz invariant, products of up to any three of the field strengths, covariant derivatives
 63 of the scalar field, and products of fermions, the geoSMEFT was formulated to include all
 64 three-point functions of SM fields plus arbitrarily many products of scalar fields [10]. This
 65 allowed for all-orders (in the SMEFT power counting) tree-level studies of the SMEFT
 66 in [11]. With all three-point functions defined to all orders in the geoSMEFT we can now
 67 use an alternative approach to studying the truncation error in the SMEFT. In [6] the
 68 full set of Z -pole observables at LEP were studied, and an alternative truncation error

69 estimate was proposed - varying the dependence on Wilson coefficients of the $1/\Lambda^4$ result
 70 in order to infer the error in the strictly $1/\Lambda^2$ terms.

71 With an enormous interest being generated around loop calculations in the SMEFT
 72 an important next obstacle for the geoSMEFT is to define a similar system for estimating
 73 truncation error at one loop. As mentioned above the geoSMEFT only includes vertices of
 74 three fields with an arbitrary number of scalar insertions. As such, the geoSMEFT is cur-
 75 rently only suitable for the calculation of the tadpole diagram. This article demonstrates
 76 the ability to calculate the tadpole at one-loop and all orders in the SMEFT power count-
 77 ing and motivates further development of the geoSMEFT in order to allow consistently
 78 defined truncation errors at both tree- and one-loop level.

79 The article is organized as follows: In Section 2 we define the conventions used in
 80 the paper as well as introduce the set of relevant operator forms which contribute to
 81 the one-loop tadpole diagram, while in Section 3 we outline the Feynman rules derived
 82 from the classical Lagrangian. In Section 4 we gauge fix the geoSMEFT and derive the
 83 Feynman rules related to gauge fixing as well as the Feynman rules for ghosts. Then
 84 in Section 5 we give the main result of this article, the all orders tadpole, and Sec. 6 is
 85 dedicated to discussion of the outlook for the one-loop geoSMEFT and conclusions. The
 86 Appendix A includes relevant definitions and relations from the geoSMEFT which are
 87 used throughout this article, while App. B demonstrates the importance of the Tadpole
 88 diagram both phenomenologically and in preserving the gauge symmetry of the theory
 89 beyond tree level.

90 2 Conventions

91 In order to define the relevant terms of the Lagrangian for the calculation of the tadpole
 92 diagram, we follow the formulation of the geoSMEFT given in [10], as well as the gauge
 93 fixing of [9] and [12]. We begin by defining the field content of the geoSMEFT, the Higgs
 94 doublet of the SM is rewritten in terms of a four-component real scalar field, ϕ^I , by the
 95 following association:

$$H(\phi_I) = \frac{1}{\sqrt{2}} \begin{bmatrix} \phi_2 + i\phi_1 \\ \phi_4 - i\phi_3 \end{bmatrix}. \quad (3)$$

96 The $SU(2)_L$ and $U(1)_Y$ gauge bosons, B and W^I , are replaced with four component vector
 97 field $W^A = \{W^1, W^2, W^3, B\}$. These weak-eigenstate fields are transformed to the mass
 98 basis by the matrices:

$$\mathcal{U}_C^A \equiv \sqrt{g}^{AB} U_{BC}, \quad \mathcal{V}_K^I \equiv \sqrt{h}^{IJ} V_{JK}. \quad (4)$$

99 Above and in what follows latin indices are four-component unless otherwise specified.
 100 The matrices \sqrt{g} and \sqrt{h} are the inverse-square root expectation value of the field-space

101 connections¹:

$$h_{IJ} = \left[1 + \phi^2 c_{H\Box}^{(6)} + \sum_{n=0}^{\infty} \left(\frac{\phi^2}{2} \right)^{n+2} (c_{HD}^{(8+2n)} - c_{H,D2}^{(8+2n)}) \right] \delta_{IJ} + \frac{\Gamma_{A,J}^I \phi^K \Gamma_{A,L}^K \phi^L}{2} \left(\frac{c_{HD}^{(6)}}{2} + \sum_{n=0}^{\infty} \left(\frac{\phi^2}{2} \right)^{n+1} c_{HD,2}^{(8+2n)} \right), \quad (5)$$

$$g_{AB} = \left[1 - 4 \sum_{n=0}^{\infty} (c_{HW}^{(6+2n)} (1 - \delta_{A4}) + c_{HB}^{(6+2n)} \delta_{A4}) \left(\frac{\phi^2}{2} \right)^{n+1} \right] \delta_{AB} - \sum_{n=0}^{\infty} \left(\frac{\phi^2}{2} \right)^n (\phi_I \Gamma_{A,J}^I \phi^J) (\phi_L \Gamma_{B,K}^L \phi^K) (1 - \delta_{A4}) (1 - \delta_{B4}) + \left[\sum_{n=0}^{\infty} c_{HWB}^{(6+2n)} \left(\frac{\phi^2}{2} \right)^n \right] [(\phi_I \Gamma_{A,J}^I \phi^J) (1 - \delta_{A4}) \delta_{B4} + (A \leftrightarrow B)]. \quad (6)$$

102 These field space connections correspond to the products of fields: $W_{\mu\nu}^A W^{B,\mu\nu}$ and
103 $(D_\mu \phi)^I (D^\mu \phi)^J$ respectively. As the scalar field ϕ is related to its mass eigenstate field
104 Φ by the inverse square roots of the expectations of these matrices, they are (in the
105 mass eigenstate basis) implicitly dependent on \sqrt{h} . The matrices U and V take the weak
106 eigenstate fields and rotate them to the physical basis of the SM, they are given by:

$$U_{BC} = \begin{bmatrix} \frac{1}{\sqrt{2}} & \frac{1}{\sqrt{2}} & 0 & 0 \\ \frac{i}{\sqrt{2}} & \frac{-i}{\sqrt{2}} & 0 & 0 \\ 0 & 0 & \bar{c}_W & \bar{s}_W \\ 0 & 0 & -\bar{s}_W & \bar{c}_W \end{bmatrix}, \quad V_{JK} = \begin{bmatrix} \frac{-i}{\sqrt{2}} & \frac{i}{\sqrt{2}} & 0 & 0 \\ \frac{1}{\sqrt{2}} & \frac{1}{\sqrt{2}} & 0 & 0 \\ 0 & 0 & -1 & 0 \\ 0 & 0 & 0 & 1 \end{bmatrix}. \quad (7)$$

107 U and V transform the weak eigenstate basis fields, W and ϕ , to the physical basis fields
108 $A^B = \{W^+, W^-, Z, A\}$ and $\Phi^I = \{\Phi^-, \Phi^+, \chi, h\}$. Note, h is used to denote the Higgs
109 boson as well as the field-space connection of Eq. 5. When the h field-space connection is
110 used it has either indices or appears as \sqrt{h} . According to the above, the bosonic fields are
111 rotated to the mass basis as:

$$A^B = \mathcal{U}_C^B W^C, \quad \Phi^I = \mathcal{V}_K^I \phi^K. \quad (8)$$

112 The barred Weinberg angles, \bar{s}_W and \bar{c}_W are defined in the Appendix. In addition to the
113 above we also have the ghosts for the electroweak gauge bosons, $u^A = \mathcal{U}_C^A u^C$, the gluon
114 field G^A and the corresponding ghost u_G^A . The gluons and their corresponding ghosts are
115 transformed to canonically normalized fields by:

$$G^A = \sqrt{\kappa^{-1}} \mathcal{G}^A, \quad u_G^A = \sqrt{\kappa^{-1}} u_{\mathcal{G}}^A. \quad (9)$$

116 κ is defined below, and is the field space connection of the combination $\mathcal{G}_{\mu\nu}^A \mathcal{G}^{A,\mu\nu}$. Script
117 latin indices are $SU(3)_c$ gluon indices. G corresponds to the canonically normalized gluonic
118 field, while \mathcal{G} corresponds to the gluonic field before the kinetic term is transformed. In
119 this article, fermionic fields only occur in loops and are therefore always summed over, as
120 such we use the short hand ψ for all fermionic fields.

121 The full set of operator forms contributing to two- and three-point functions of the

¹Raised indices on field-space connections correspond to inverses of the field-space connection.

122 SMEFT was derived in [10]. They include:

$$\begin{aligned}
& h_{IJ}(D_\mu\phi)^I(D_\mu\phi)^J, & g_{AB}W_{\mu\nu}^AW^{B\mu\nu}, & \kappa_{IJ}^A(D_\mu\phi)^I(D_\nu\phi)^JW_A^{\mu\nu}, \\
& \mathcal{Y}^\psi\bar{\psi}_1\psi_2, & \kappa\mathcal{G}_{\mu\nu}^A\mathcal{G}^{A\mu\nu}, & \\
& f_{ABC}W_{\mu\nu}^AW^{B,\nu\rho}W_\rho^{C,\mu}, & d_A\bar{\psi}_1\sigma^{\mu\nu}\psi_2\mathcal{W}_{\mu\nu}^A, & \kappa_{ABC}\mathcal{G}_{\mu\nu}^A\mathcal{G}^{B,\nu\rho}\mathcal{G}_\rho^{C,\mu}, \\
& c\bar{\psi}_1\sigma^{\mu\nu}T_A\psi_2\mathcal{G}_{\mu\nu}^A, & L_{IA}\bar{\psi}_1\gamma^\mu\sigma_A\psi_2(D_\mu\phi)^I. &
\end{aligned} \tag{10}$$

123 The covariant derivative of the four component scalar and the field strength tensors of the
124 vectors are then defined as:

$$(D_\mu\phi)^I = \left(\partial^\mu\delta_J^I - \frac{1}{2}W^{A,\mu}\tilde{\gamma}_{A,J}^I \right) \phi^J, \tag{11}$$

$$W_{\mu\nu}^A = \partial_\mu W_\nu^A - \partial_\nu W_\mu^A - \tilde{\epsilon}^A_{BC}W_\mu^B W_\nu^C, \tag{12}$$

$$\mathcal{G}_{\mu\nu}^A = \partial_\mu\mathcal{G}_\nu^A - \partial_\nu\mathcal{G}_\mu^A - f^A_{BC}\mathcal{G}_\mu^B\mathcal{G}_\nu^C. \tag{13}$$

125 The matrices $\tilde{\gamma}_{A,J}^I$ and $\tilde{\epsilon}^A_{BC}$ are defined in the Appendix. The f^A_{BC} are the usual structure
126 constants of $SU(3)_c$.

127 In addition to the operators defined in Eq. 10 we also define the all-orders Higgs
128 potential,

$$V(\phi^I) = \frac{\lambda}{4}(\phi^2 - v_0^2)^2 - \sum_{n=1}^{\infty} c_H^{(4+2n)} \left(\frac{\phi^2}{2} \right)^{2+n}. \tag{14}$$

129 In the above, v_0 is the vacuum expectation value that minimizes the tree-level Higgs
130 potential for the SM. Spontaneous symmetry breaking occurs in the geoSMEFT for $\phi^I \rightarrow$
131 $v\delta^{I4} + \sqrt{h}^{IJ}V_{JK}\Phi^{K2}$, where v is the vacuum expectation value which minimizes the tree
132 level potential of the geoSMEFT. $c_H^{(4+2n)}$ is the Wilson coefficient of the dimension $4+2n$
133 pure Higgs operator suppressed by the heavy mass scale Λ^{2n} , this Λ dependence is absorbed
134 into the Wilson coefficient here and for the operators below for convenience. At tree level,
135 requiring the coefficient of the tadpole term in the potential be zero gives the relation
136 between v_0 and v :

$$t = 0 \propto v^2 - \frac{1}{\lambda} \sum_{n=1}^{\infty} \frac{(4+2n)v^{2+2n}}{2^{2+n}} c_H^{(2n+4)} - v_0^2. \tag{15}$$

137 We note that solving this equation for v^2 requires numerical methods for $n \geq 4$ as it is a
138 polynomial of order $n+1$ in v^2 .

139 In what follows we will derive the one-loop correction to this result to all orders in the
140 SMEFT power counting. The choice of $t = 0$ at one loop corresponds to the FJ tadpole
141 scheme [13], with this choice we choose to expand about the true (one-loop) vacuum. This
142 simplifying choice means tadpole diagrams need not be included in one-loop calculations
143 (the tadpole and its counter term exactly cancel), however the loop improved vacuum
144 expectation value needs to be used in tree level calculations. Further, this one-loop result
145 is required to demonstrate the gauge invariance of observables, such as the masses of
146 the gauge bosons in the on-shell renormalization scheme [14, 15]. This is discussed in
147 Appendix B as well as in the conclusions.

148 The terms from Eq. 10 which contribute to the one-loop tadpole diagram are those
149 which involve a single Higgs boson coupling to two fermions, gauge bosons, or additional

²This is a convenient choice of how to realize spontaneous symmetry breaking in the geoSMEFT which is consistent with $\langle H^\dagger H \rangle = v^2/2$ [12].

150 scalars. As such the last two lines do not contribute as they include three or more particles
 151 other than the Higgs boson and therefore only contribute at higher loop order. In the
 152 case of the connection L_{IA} there is no contribution as these operators correspond to the
 153 Hermitian derivative form, $(H^\dagger \overleftrightarrow{D}_\mu H)(\bar{\psi}\gamma^\mu\psi)$, which causes the Higgs-fermion couplings
 154 to vanish identically. While the operators coupling the Higgs boson to gluons will result in
 155 scale-less loop integrals which vanish identically, we retain them as the all-orders Feynman
 156 rules derived from the $\kappa_{\mathcal{A}\mathcal{B}}$ operator form are the simplest and serve as intuitive examples
 157 of how the rules are derived. Reproducing the all-orders form of the relevant connections
 158 from [10] we have (in addition to Eqs. 5 and 6 above):

$$\begin{aligned} \kappa_{IJ}^A &= -\frac{1}{2}\gamma_{4,J}^I\delta_{A4}\sum_{n=0}^{\infty}c_{HDHB}^{(8+2n)}\left(\frac{\phi^2}{2}\right)^{n+1}-\frac{1}{2}\gamma_{A,J}^I(1-\delta_{A4})\sum_{n=0}^{\infty}c_{HDHW}^{(8+2n)}\left(\frac{\phi^2}{2}\right)^{n+1} \\ &\quad -\frac{1}{8}(1-\delta_{A4})[\phi_K\Gamma_{A,L}^K\phi^L][\phi_M\Gamma_{B,L}^M\phi^N]\gamma_{B,J}^I\sum_{n=0}^{\infty}c_{HDHW,3}^{(10+2n)}\left(\frac{\phi^2}{2}\right)^n \\ &\quad +\frac{1}{4}\epsilon_{ABC}[\phi_K\Gamma_{B,L}^K\phi^L]\gamma_{C,J}^I\sum_{n=0}^{\infty}c_{HDHW,2}^{(8+2n)}\left(\frac{\phi^2}{2}\right)^n, \end{aligned} \quad (16)$$

$$\mathcal{Y}_{pr}^\psi = -\overset{(\sim)}{H}(\phi_I)[Y_\psi]^\dagger + \overset{(\sim)}{H}(\phi_I)\sum_{n=0}^{\infty}c_{\psi H,pr}^{(6+2n)}\left(\frac{\phi^2}{2}\right)^{n+1}, \quad (17)$$

$$\kappa = \left[1 - 4\sum_{n=0}^{\infty}c_{HG}^{(6+2n)}\left(\frac{\phi^2}{2}\right)^{n+1}\right]. \quad (18)$$

159

160 Where $\overset{(\sim)}{H}$ is the Higgs doublet for leptons and down quarks, and $\epsilon_{ij}H^j$ for up quarks.
 161 The matrices $\Gamma_{A,J}^I$ and $\gamma_{A,J}^I$ are given in the Appendix for brevity. We have also used
 162 $\phi^2 = \phi^I\phi_I = \phi_I\delta^{IJ}\phi_J$. The $c_i^{(n)}$ are the Wilson coefficients of operators of dimension n
 163 and are suppressed by a factor of Λ^{n-4} which has been absorbed into their definition for
 164 the sake of compactness of these and the following expressions. The inverse-square root
 165 of g_{IJ} and h_{IJ} are the matrices of Eq. 4 which, with the matrices U and V , take the
 166 weak eigenstate fields to the mass eigenstate fields of the SMEFT. Latin indices A, B, \dots
 167 are those associated with the four-component representation of the gauge boson indices
 168 for $SU(2)_L \times U(1)_Y$, I, J, \dots are the four-component indices associated with the
 169 four-component real scalar field, and \mathcal{A}, \mathcal{B} are associated with color indices of the gluons.
 170 Fermionic indices are generally suppressed.

171 The above is all that is needed to define the relevant all-orders three-point functions
 172 for the classical Lagrangian in the geoSMEFT:

$$\begin{aligned} \mathcal{L}_{\text{cl}}(\phi^I, W^A, \mathcal{G}^A, \psi) &= h_{IJ}(D_\mu\phi)^I(D_\mu\phi)^J - V(\phi) + g_{AB}W_{\mu\nu}^AW^{B,\mu\nu} + \kappa\mathcal{G}_{\mu\nu}^A\mathcal{G}^{A,\mu\nu} \\ &\quad + \kappa_{IJ}^A(D_\mu\phi)^I(D_\nu\phi)^JW_A^{\mu\nu} + \sum_{\psi}\mathcal{Y}\bar{\psi}_1\psi_2. \end{aligned} \quad (19)$$

173 In Section 4 we will choose to adopt the background field method of gauge fixing. Therefore
 174 in the discussion of the classical Lagrangian that follows we will double the bosonic field
 175 content of the above Lagrangian as:

$$\mathcal{L}_{\text{cl}}(\phi^I, W_\mu^A, \mathcal{G}_\mu^A, \psi) \rightarrow \mathcal{L}_{\text{cl}}(\phi^I + \hat{\phi}^I, W^A + \hat{W}^A, \mathcal{G}^A + \hat{\mathcal{G}}^A, \psi). \quad (20)$$

176 Where the hatted fields are referred to as the background fields and the unhatted as the
 177 quantum fields. The choice of the background field method has various advantages, one
 178 of which is the preservation of the naive Ward Identities as discussed in [12, 16, 17]. This
 179 methodology has been adopted in many SMEFT related publications because of its nice

180 properties, see for example [7, 18, 19]. In this methodology the quantum fields are gauge
 181 fixed, while the background fields are not. As fermionic fields are not involved in the
 182 gauge fixing they are not split into background and quantum fields. As such all external
 183 particles for a given amplitude correspond to background field while internal lines are
 184 quantum fields. Therefore in what follows we derive the couplings of the background
 185 Higgs boson field, \hat{h} , to two quantum fields.

186 3 The all-orders vertices

187 In order to define the relevant three-point functions for the one-loop tadpole diagrams we
 188 must obtain the relevant Feynman rules from Eq. 10. We will do this while preserving
 189 the form of the field-space connections when possible in order to maintain results that
 190 are manifestly all orders in the $\frac{1}{\Lambda^n}$ power counting. The Feynman rules that follow were
 191 checked using `FeynRules`. They can be understood as follows: the subscript of a field in $\{\}$
 192 corresponds to the momenta, Lorentz indices, and color indices with the same subscript
 193 on the right side of the equations below. In the case of a field with no subscript, the
 194 Feynman rule does not depend explicitly on that field's properties.

195 The simplest Feynman rules to derive are from the field space connections g_{AB} , κ_{AB} ,
 196 and Y_{pr}^ψ as the Higgs dependence is purely in the connection matrix. Varying Eq. 18 with
 197 respect to the background field \hat{h} gives the coupling of a Higgs boson to two gluons:

$$\{\hat{h}, G_1, G_2\} = i \left\langle \frac{\delta \kappa}{\delta \hat{h}} \right\rangle \left(\sqrt{\kappa^{-1}} \right)^2 \Pi_{1,2} \delta^{A_1 A_2}. \quad (21)$$

198 Where, for convenience, we have defined,

$$\Pi_{1,2} \equiv (p_1^{\mu_2} p_2^{\mu_1} - p_1 \cdot p_2 \eta^{\mu_1 \mu_2}). \quad (22)$$

199 It should be noted there are implied rotations of the quantity ϕ_I within the field-space
 200 connections such as κ : beyond leading order $\sqrt{\kappa}$ is a function of $\phi^I = \sqrt{\hat{h}}^{IJ} V_{JK} \Phi^K$.
 201 Explicitly taking the variations gives instead:

$$\{\hat{h}, G_1, G_2\} \rightarrow i \sqrt{\hat{h}}^{44} \left(\sqrt{\kappa^{-1}} \right)^2 v_T \sum_{i=0}^{\infty} \frac{v_T^{2n} (n+1)}{2^{n-2}} c_{HG}^{(6+2n)} \Pi_{1,2} \delta^{A_1 A_2}. \quad (23)$$

202 Similarly for the yukawa-like couplings:

$$\{\hat{h}, \bar{\psi}_r, \psi_r\} = -i \left\langle \frac{\delta \mathcal{Y}_{rr}^\psi}{\delta \hat{h}} \right\rangle \quad (24)$$

$$= i \frac{\sqrt{\hat{h}}^{44}}{v} \bar{M}_{\psi,rr} - i \frac{\sqrt{\hat{h}}^{44}}{\sqrt{2}} \sum_{n=0}^{\infty} c_{\psi H,rr}^{(6+2n)} \frac{v^{2n+2}}{2^{n+1}} (2n+2). \quad (25)$$

203 As only like-flavors will contribute to the Tadpole diagram we have only considered diago-
 204 nal entries of \mathcal{Y}^ψ and substituted in terms of the barred tree-level masses of the fermions.
 205 The tree-level fermion mass to all orders is simply the expectation of the field connection
 206 \mathcal{Y} of Eq. 17:

$$\bar{M}_\psi = \langle (\mathcal{Y}^\psi)^\dagger \rangle. \quad (26)$$

207 The remaining terms are more complicated than the above, as such we only write the
 208 vertex functions in terms of variations on the field-space connections. Some examples of

209 the field-space connections expanded in terms of Wilson coefficients can be found in the
210 Appendix. The coupling to two gauge bosons coming from g_{AB} is given by:

$$\{\hat{h}, W_1^+, W_2^-\} = -i \left\langle \frac{\delta g_{11}}{\delta \hat{h}} \right\rangle (\sqrt{g}^{11})^2 \Pi_{1,2}, \quad (27)$$

$$\{\hat{h}, A_1, A_2\} = -i \Sigma_{AA} \Pi_{1,2}, \quad (28)$$

$$\{\hat{h}, Z_1, Z_2\} = -i \Sigma_{ZZ} \Pi_{1,2}, \quad (29)$$

$$\Sigma_{AA} \equiv \sum_{A,B=3}^4 \left(\bar{c}_W^2 \left\langle \frac{\delta g_{AB}}{\delta \hat{h}} \right\rangle \sqrt{g}^{A4} \sqrt{g}^{B4} + 2\bar{c}_W \bar{s}_W \left\langle \frac{\delta g_{AB}}{\delta \hat{h}} \right\rangle \sqrt{g}^{3A} \sqrt{g}^{B4} + \bar{s}_W^2 \left\langle \frac{\delta g_{AB}}{\delta \hat{h}} \right\rangle \sqrt{g}^{3A} \sqrt{g}^{3B} \right), \quad (30)$$

$$\begin{aligned} \Sigma_{ZZ} &\equiv \sum_{A,B=3}^4 \left(\bar{c}_W^2 \left\langle \frac{\delta g_{AB}}{\delta \hat{h}} \right\rangle \sqrt{g}^{3A} \sqrt{g}^{3B} - 2\bar{c}_W \bar{s}_W \left\langle \frac{\delta g_{AB}}{\delta \hat{h}} \right\rangle \sqrt{g}^{3A} \sqrt{g}^{B4} + \bar{s}_W^2 \left\langle \frac{\delta g_{AB}}{\delta \hat{h}} \right\rangle \sqrt{g}^{A4} \sqrt{g}^{B4} \right) \\ &= \Sigma_{AA} (\bar{s}_W \rightarrow -\bar{c}_W, \bar{c}_W \rightarrow \bar{s}_W). \end{aligned} \quad (31)$$

211

212 In order to form a tadpole diagram from the connection κ_{IJ}^A one of the covariant deriva-
213 tives must generate a vector boson while the other must correspond to the background
214 Higgs boson, as such the rules are straightforward to derive as well:

$$\begin{aligned} \{\hat{h}_1, W_2^+, W_3^-\} &= \bar{g}_2 \sqrt{g}^{11} \sqrt{h}^{44} v \left[(\langle \kappa_{13}^1 \rangle - i \langle \kappa_{14}^1 \rangle) p_1^{\mu_2} p_2^{\mu_3} - (\langle \kappa_{13}^1 \rangle + i \langle \kappa_{14}^1 \rangle) p_1^{\mu_3} p_3^{\mu_2} \right. \\ &\quad \left. + (\langle \kappa_{13}^1 \rangle [p_1 \cdot p_3 - p_1 \cdot p_2] + i \langle \kappa_{14}^1 \rangle [p_1 \cdot p_2 + p_1 \cdot p_3]) \eta^{\mu_2 \mu_3} \right], \end{aligned} \quad (32)$$

$$\begin{aligned} \{\hat{h}_1, Z_2, Z_3\} &= -i \sqrt{h}^{44} \bar{g}_2 v \left[(\bar{c}_W \sqrt{g}^{33} - \bar{s}_W \sqrt{g}^{34}) \langle \kappa_{34}^3 \rangle + (\bar{s}_W \sqrt{g}^{44} - \bar{c}_W \sqrt{g}^{34}) \langle \kappa_{12}^4 \rangle \right] \\ &\quad \times [p_1^{\mu_2} p_2^{\mu_3} + p_1^{\mu_3} p_3^{\mu_2} - p_1 \cdot (p_2 + p_3) \eta^{\mu_2 \mu_3}]. \end{aligned} \quad (33)$$

215 No coupling to the photon is generated as one of the vector bosons must come from the
216 covariant derivative which has no A dependence for the Higgs boson. In simplifying these
217 expressions we have used:

$$\langle \kappa_{13}^1 \rangle = -\langle \kappa_{24}^1 \rangle = -\langle \kappa_{31}^1 \rangle = \langle \kappa_{42}^1 \rangle = \langle \kappa_{14}^2 \rangle = \langle \kappa_{23}^2 \rangle = -\langle \kappa_{32}^2 \rangle = -\langle \kappa_{41}^2 \rangle, \quad (34)$$

$$\langle \kappa_{14}^1 \rangle = \langle \kappa_{23}^1 \rangle = -\langle \kappa_{32}^1 \rangle = -\langle \kappa_{41}^1 \rangle = -\langle \kappa_{13}^2 \rangle = \langle \kappa_{24}^2 \rangle = \langle \kappa_{31}^2 \rangle = -\langle \kappa_{42}^2 \rangle, \quad (35)$$

$$\langle \kappa_{12}^4 \rangle = -\langle \kappa_{34}^4 \rangle. \quad (36)$$

218 In addition to the fact κ_{IJ}^A is antisymmetric. As the rules for interactions derived from
219 κ_{IJ}^A necessarily depend on the momentum of the background Higgs boson (i.e. one of
220 the derivatives must be acting on the Higgs boson) these rules will not contribute to the
221 tadpole diagram.

222 Finally, the Feynman rules arising from the field-space connection h_{IJ} are slightly more
223 complicated as the background Higgs boson can come from either the metric or the $(D_\mu \phi)$
224 terms. These operator forms also contribute not only to Higgs-gauge couplings, but also
225 to Higgs-goldstone couplings. For \hat{h} sourced from the field space connection we have the

226 following rules:

$$\{\hat{h}, \Phi_1^0, \Phi_1^0\} = -i \left\langle \frac{\delta h_{33}}{\delta \hat{h}} \right\rangle (\sqrt{h}^{33})^2 p_1 \cdot p_2, \quad (37)$$

$$\{\hat{h}, \Phi_1^+, \Phi_2^-\} = -i \left\langle \frac{\delta h_{11}}{\delta \hat{h}} \right\rangle (\sqrt{h}^{11})^2 p_1 \cdot p_2, \quad (38)$$

$$\{\hat{h}, h_1, h_2\} = -i \left\langle \frac{\delta h_{44}}{\delta \hat{h}} \right\rangle (\sqrt{h}^{44})^2 p_1 \cdot p_2, \quad (39)$$

$$\{\hat{h}, W_1^+, W_2^-\} = i \left\langle \frac{\delta h_{11}}{\delta \hat{h}} \right\rangle \bar{M}_W^2 (\sqrt{h}^{11})^2 \eta_{\mu_1 \mu_2}, \quad (40)$$

$$\{\hat{h}, Z_1, Z_2\} = i \left\langle \frac{\delta h_{33}}{\delta \hat{h}} \right\rangle \bar{M}_Z^2 (\sqrt{h}^{33})^2 \eta_{\mu_1 \mu_2}. \quad (41)$$

227 The coupling $\hat{h}\gamma\gamma$ vanishes identically, which follows from the fact the operator forms
 228 of the field-space connection h_{IJ} correspond to rescalings of the SM Higgs couplings to
 229 vector bosons. In the case that \hat{h} is sourced from the covariant derivative terms we have
 230 two contributions. The first is from the $\langle h \rangle$ which can only generate \hat{h} -vector three point
 231 functions³:

$$\{\hat{h}, W_1^+, W_2^-\} = 2i\sqrt{h}^{44} \frac{\bar{M}_W^2}{v} \eta_{\mu_1 \mu_2}, \quad (42)$$

$$\{\hat{h}, Z_1, Z_2\} = 2i\sqrt{h}^{44} \frac{\bar{M}_Z^2}{v} \eta_{\mu_1 \mu_2}. \quad (43)$$

232 As above, the $\hat{h}\gamma\gamma$ coupling vanishes identically. Secondly, \hat{h} couplings to goldstone bosons
 233 from variations of the metric with respect to the goldstone bosons could be present, how-
 234 ever they vanish identically.

235 In addition to the above we need to include terms like $c_H^{(2n-4)}(H^\dagger H)^{2n}$. The Feynman
 236 rules for \hat{h} coupling to two quantum fields can be generalized from Eq. 4.2 of [10] by using
 237 the multinomial coefficient:

$$\{\hat{h}, h, h\} = -2i(\sqrt{h}^{44})^3 v \left[3\lambda - \sum_{n=3}^{\infty} \frac{1}{2^n} \binom{2n}{1, 2, 2n-3} v^{2n-4} c_H^{(2n)} \right], \quad (44)$$

$$\{\hat{h}, \Phi^0, \Phi^0\} = -2i(\sqrt{h}^{33})^2 \sqrt{h}^{44} v \left[\lambda - \sum_{n=3}^{\infty} \frac{1}{2^{n-1}} \binom{n}{1, 1, n-2} v^{2n-4} c_H^{(2n)} \right], \quad (45)$$

$$\{\hat{h}, \Phi^+, \Phi^-\} = -i(\sqrt{h}^{11})^2 \sqrt{h}^{44} v \left[2\lambda - \sum_{n=3}^{\infty} \frac{1}{2^{n-2}} \binom{n}{1, 1, n-2} v^{2n-4} c_H^{(2n)} \right]. \quad (46)$$

238 In the above the multinomial for $\hat{h}h^2$ can be understood to come from $(v + \hat{h} + h)^{2n}$ terms,
 239 the Φ^0 rule from $[(\Phi^0)^2 + 2\hat{h}v + v^2]^n$, and the rule for Φ^\pm from $[2|\Phi^\pm|^2 + 2\hat{h}v + v^2]^n$. This
 240 explains the minor differences between the Feynman rules above.

241 The above constitute all the rules from the classical Lagrangian necessary to perform
 242 the calculation of the tadpole diagrams to all orders in the SMEFT power counting, what
 243 remains are the gauge-fixing and ghost contributions.

244 4 Gauge fixing the geoSMEFT

245 Background gauge fixing for the SMEFT was performed first in [9]. This was first done for
 246 the gluons in [18], then later repeated in [16] in a manner more consistent with the gauge

³Also $\hat{h}\Phi^{0,\pm}$ -vector couplings which do not contribute to the Tadpole diagram.

247 fixing of the weak gauge bosons of [9] which is adopted here. The gauge fixing terms are
248 given by:

$$\mathcal{L}_{GF} = -\frac{\hat{g}_{AB}}{2\xi_W}\mathcal{G}^A\mathcal{G}^B - \frac{\kappa}{2\xi_G}\mathcal{G}_{\text{color}}^A\mathcal{G}_{\text{color}}^A, \quad (47)$$

$$\mathcal{G}^A = \partial_\mu W^{A,\mu} - \tilde{e}^A{}_{BC}\hat{W}_\mu^B W^{C\mu} + \frac{\xi}{2}\hat{g}^{AB}\phi^I\hat{h}_{IK}\tilde{\gamma}_{B,J}^K\hat{\phi}^J, \quad (48)$$

$$\mathcal{G}_{\text{color}}^A = \partial_\mu G^{\mu,A} - g_3 f^{ABC}\hat{G}_{\mu,B}G_C^\mu. \quad (49)$$

249 Where in the above, unhatted fields are understood to be quantum fields and the hatted
250 field-space connections are the normal field space connections (i.e. \hat{g} and \hat{h}) with all
251 quantum fields set to zero. This notational choice is also the case below in the ghost
252 Lagrangian. Starting with the gluonic gauge fixing as it is the simplest we obtain the
253 Feynman rule:

$$\{\hat{h}, G_1, G_2\} = \frac{i}{\xi_G} \left\langle \frac{\delta\kappa}{\delta\hat{h}} \right\rangle (\sqrt{\kappa^{-1}})^2 p_1^{\mu_1} p_2^{\mu_2} \delta^{A_1 A_2}. \quad (50)$$

254 In the case of the electroweak gauge fixing a coupling of the background Higgs field to gauge
255 bosons can be obtained from the variation with respect to the field-space connection of
256 Eq. 47 and the square of the derivative term of Eq. 48. The second terms of Eqs. 48 and 49
257 cannot contribute as they include a background gauge field, while the final term allows
258 for a \hat{h} coupling to goldstone bosons when all but one of the \hat{g} , \hat{h} , and $\hat{\phi}$ are set to their
259 expectation values. This results in the following Feynman Rules:

$$\{\hat{h}, W_1^+, W_2^-\} = \frac{i}{\xi_W} \left\langle \frac{\delta g_{11}}{\delta\hat{h}} \right\rangle (\sqrt{g^{11}})^2 p_1^{\mu_1} p_2^{\mu_2}, \quad (51)$$

$$\{\hat{h}, A_1, A_2\} = \frac{i}{\xi_W} \Sigma_{AA} p_1^{\mu_1} p_2^{\mu_2}, \quad (52)$$

$$\{\hat{h}, Z_1, Z_2\} = \frac{i}{\xi_W} \Sigma_{ZZ} p_1^{\mu_1} p_2^{\mu_2}, \quad (53)$$

$$\{\hat{h}, \Phi^+, \Phi^-\} = -i \frac{\bar{M}_W^2}{v} \left[2 \left\langle \frac{\delta h_{11}}{\delta\hat{h}} \right\rangle (\sqrt{h^{11}})^2 v + 2\sqrt{h^{44}} + \left\langle \frac{\delta g^{11}}{\delta\hat{h}} \right\rangle (\sqrt{g_{11}})^2 v \right] \xi_W \quad (54)$$

$$\{\hat{h}, \Phi^0, \Phi^0\} = -i \frac{\bar{M}_Z^2}{v} \left[2 \left\langle \frac{\delta h_{33}}{\delta\hat{h}} \right\rangle (\sqrt{h^{33}})^2 v + 2\sqrt{h^{44}} - \Sigma_{ZZ} v \right] \xi_W. \quad (55)$$

$$(56)$$

260 Note no \hat{h} coupling to two quantum Higgs bosons is generated.

261 The ghost Lagrangian was also derived in [9]⁴, it is reproduced here excluding any
262 terms with gauge fields as they cannot contribute to the one-loop Tadpole diagram (the
263 ghost Lagrangian is by definition quadratic in the ghost fields):

$$\mathcal{L}_{\text{ghost}} = -\hat{g}_{AB}\bar{u}^B \left[\partial^2 + \frac{\xi_W}{4}\hat{g}^{AD}(\phi^J + \hat{\phi}^J)\tilde{\gamma}_{CJ}^I\hat{h}_{IK}\tilde{\gamma}_{DL}^K\hat{\phi}^L \right] u^C - \hat{\kappa}\bar{u}_A^G\partial^2 u_A^G. \quad (57)$$

264 As was the case for the gauge fixing terms, $\hat{h}\bar{u}u$ couplings can be obtained either from a

⁴Here we have adopted the sign choice of [18].

265 variation with respect to one of the field-space connections or explicitly from $\hat{\phi}$, \hat{h} , or \hat{g} :

$$\{\hat{h}, \bar{u}_1^G, u_2^G\} = i \left\langle \frac{\delta \kappa}{\delta \hat{h}} \right\rangle (\sqrt{\kappa^{-1}})^2 p_2^2 \delta_{A_1 A_2}, \quad (58)$$

$$\{\hat{h}, \bar{u}_1^{W^+}, u_2^{W^+}\} = -i \left[\left\langle \frac{\delta h_{11}}{\delta \hat{h}} \right\rangle \bar{M}_W^2 (\sqrt{h^{11}})^2 \xi + 2 \bar{M}_W^2 \sqrt{h^{44}} \xi - (\sqrt{g^{11}})^2 \left\langle \frac{\delta g_{11}}{\delta \hat{h}} \right\rangle p_2^2 \right] \quad (59)$$

$$= \{\hat{h}, \bar{u}_1^{W^-}, u_2^{W^-}\}, \quad (60)$$

$$\{\hat{h}, \bar{u}_1^\gamma, u_2^\gamma\} = i \Sigma_{AA} p_2^2,$$

$$\{\hat{h}, \bar{u}_1^Z, u_2^Z\} = i \Sigma_{ZZ} p_2^2 - i \bar{M}_Z^2 \left(2 \sqrt{h^{44}} + (\sqrt{h^{33}})^2 \left\langle \frac{\delta h_{33}}{\delta \hat{h}} \right\rangle \right) \xi. \quad (61)$$

266 In the case of the ghosts associated with the photon, the ξ dependent term vanishes
 267 identically. This is analogous to the case of the classical contribution from the field space
 268 metric h_{IJ} , see the discussions around Eqs. 41 and 43. Note that in the case of the ghost
 269 for the photon field we have used the notation u^γ to distinguish the field from the four-
 270 component ghost field u^A . With the above, all Feynman rules necessary to calculate the
 271 tadpole diagram at one loop and to all orders in the SMEFT expansion are now defined.

272 5 The all-orders SMEFT tadpole

273 The one loop diagrams that contribute are shown in Figure 1, as was noted in Section 2
 274 the Feynman rules coupling the Higgs boson to gluons as well as those coupling the Higgs
 275 boson to colored ghosts do not contribute to the tadpole diagram as the loop integral is
 276 scaleless. Making use of dimensional regularization in $d = 4 - 2\epsilon$ dimensions, the fermionic
 277 couplings result in the following contribution at one loop:

$$T_H^\psi = -\frac{N_c \bar{M}_\psi}{4\pi^2} \left\langle \frac{\delta \mathcal{Y}^\psi}{\delta \hat{h}} \right\rangle A_0(\bar{M}_\psi) \quad (62)$$

$$= \frac{N_c \bar{M}_\psi}{4\pi^2} \sqrt{h^{44}} \left(\frac{\bar{M}_\psi}{v} - \frac{1}{\sqrt{2}} \sum_{n=0}^{\infty} \frac{v^{2n+2}}{2^{n+1}} (2n+2) c_{\psi H}^{(n)} \right) A_0(\bar{M}_\psi) \quad (63)$$

$$= \frac{N_c \bar{M}_\psi}{4\pi^2} \left[\frac{\bar{M}_\psi}{v} - \frac{v}{4} \left(2\sqrt{2} v c_{\psi H}^{(6)} + \bar{M}_\psi [c_{HD}^{(6)} - 4c_{H\Box}] \right) - \frac{v^4}{8} \sqrt{2} \left(c_{\psi H}^{(8)} + [4c_{H\Box}^{(6)} - c_{HD}^{(6)}] c_{\psi H}^{(6)} \right) \right. \\ \left. + \frac{\bar{M}_\psi}{32} \left(4c_{HD}^{(8)} + 4c_{HD,2}^{(8)} - 3[c_{HD}^{(6)} - 4c_{H\Box}^{(6)}]^2 \right) \right] A_0(\bar{M}_\psi) + \mathcal{O}\left(\frac{1}{\Lambda^6}\right). \quad (64)$$

278 Where we have used the Passarino-Veltman scalar A function,

$$A_0(M) = M^2 \left[1 + \frac{1}{\epsilon} - \gamma_E + \log\left(\frac{4\pi\mu^2}{M^2}\right) \right]. \quad (65)$$

279 The three equivalences of Eq. 64 show first the geoSMEFT result, the result with the
 280 variation of the field-space connection written explicitly in terms of the relevant Wilson

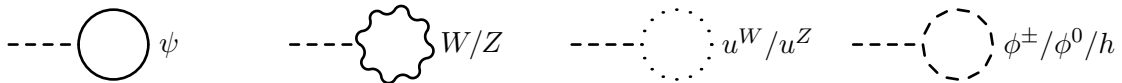


Figure 1: One loop diagrams contributing to the Tadpole. The photon and gluons and their corresponding ghosts do not contribute as they are massless the loop integrals are identically zero.

281 coefficients while keeping the compact form for the transformations that canonically nor-
 282 malizes the Higgs background field, and finally the full expansion in terms of the Wilson
 283 coefficients to order $\frac{1}{\Lambda^4}$. The barred quantities are not expanded as they are more closely
 284 related to input parameters that would be chosen in a phenomenological study, this also
 285 serves to simplify the expressions so they fit in paper format. This demonstrates that the
 286 geoSMEFT trivially sums the Wilson coefficient dependence of the SMEFT. In a tradi-
 287 tional SMEFT approach one would enumerate all the contributing operators to a given
 288 order in the SMEFT power counting and the corresponding Feynman rules, perform the
 289 calculations, and again expand to a given order. Here we perform the all orders calculation
 290 and can expand to a given order after the full calculation is performed.

291 The compactness of the expressions also allows for a cleaner understanding of cancel-
 292 lations in the theory such as in the case of cancellations between gauge-boson, ghost, and
 293 goldstone boson contributions as we see next. Below we neglect to expand in terms of
 294 individual Wilson coefficients until the terms are added together as many simplifications
 295 occur after summing the diagrams. In the case of the W and Z bosons we have:

$$T_H^W = \frac{\bar{M}_W^2}{16\pi^2} \left[(\sqrt{g^{11}})^2 \left\langle \frac{\delta g_{11}}{\delta \hat{h}} \right\rangle - \frac{2}{v} \sqrt{h^{44}} - \left\langle \frac{\delta h_{11}}{\delta \hat{h}} \right\rangle (\sqrt{h^{11}})^2 \right] \left[2\bar{M}_W^2 - 3A_0(\bar{M}_W) - \xi_W A_0(\sqrt{\xi_W} \bar{M}_W) \right], \quad (66)$$

$$T_H^Z = \frac{\bar{M}_Z^2}{32\pi^2} \left[\Sigma_{ZZ} - \frac{2}{v} \sqrt{h^{44}} - \left\langle \frac{\delta h_{33}}{\delta \hat{h}} \right\rangle (\sqrt{h^{33}})^2 \right] \left[2\bar{M}_Z^2 - 3A_0(\bar{M}_Z) - \xi A_0(\sqrt{\xi} \bar{M}_Z) \right]. \quad (67)$$

296

297 The ghost terms give (again, as the photon ghost term is scaleless the contribution is
 298 identically zero):

$$T_H^{u^\pm} = \frac{\bar{M}_W^2}{8\pi^2} \left[\left\langle \frac{\delta g_{11}}{\delta \hat{h}} \right\rangle (\sqrt{g^{11}})^2 - \frac{2}{v} \sqrt{h^{44}} - \left\langle \frac{\delta h_{11}}{\delta \hat{h}} \right\rangle (\sqrt{h^{11}})^2 \right] \xi_W A_0(\sqrt{\xi_W} \bar{M}_W), \quad (68)$$

$$T_H^{u^Z} = \frac{\bar{M}_Z^2}{16\pi^2} \left[\Sigma_{ZZ} - \frac{2}{v} \sqrt{h^{44}} - \left\langle \frac{\delta h_{33}}{\delta \hat{h}} \right\rangle (\sqrt{h^{33}})^2 \right] \xi_W A_0(\sqrt{\xi_W} \bar{M}_Z), \quad (69)$$

299 and for the goldstone bosons we find:

$$T_H^{\Phi^\pm} = \frac{\bar{M}_W^2}{16\pi^2} \left[\frac{2}{v} \sqrt{h^{44}} + \left\langle \frac{\delta h_{11}}{\delta \hat{h}} \right\rangle (\sqrt{h^{11}})^2 + \left\langle \frac{\delta g^{11}}{\delta \hat{h}} \right\rangle (\sqrt{g^{11}})^2 \right] \xi_W A_0(\sqrt{\xi_W} \bar{M}_W) \quad (70)$$

$$+ \frac{v}{32\pi^2} (\sqrt{h^{11}})^2 \sqrt{h^{44}} \left(4\lambda - \sum_{n=3}^{\infty} \frac{1}{2^{n-3}} \binom{n}{1, 1, n-2} v^{2n-4} c_H^{(2n)} \right) A_0(\sqrt{\xi_W} \bar{M}_W),$$

$$T_H^{\Phi^0} = \frac{\bar{M}_Z^2}{32\pi^2} \left[\frac{2}{v} \sqrt{h^{44}} + \left\langle \frac{\delta h_{33}}{\delta \hat{h}} \right\rangle (\sqrt{h^{33}})^2 - \Sigma_{ZZ} \right] \xi_W A_0(\sqrt{\xi_W} \bar{M}_Z) \quad (71)$$

$$+ \frac{v}{64\pi^2} (\sqrt{h^{33}})^2 \sqrt{h^{44}} \left(4\lambda - \sum_{n=3}^{\infty} \frac{1}{2^{n-3}} \binom{n}{1, 1, n-2} v^{2n-4} c_H^{(2n)} \right) A_0(\sqrt{\xi} \bar{M}_Z).$$

300

301 Noting the raised indices in δg^{11} for the Φ^\pm contribution, we see that the ξ_W dependent
 302 parts of the W and Z loops are cancelled exactly by the ghost and goldstone terms,
 303 and only the λ and $c_H^{(n)}$ gauge-parameter dependent terms remain for the scalars. This
 304 is exactly as was found for the SM Tadpole in the background field methodology [7].
 305 Interestingly, the behavior goes beyond the SM-like interactions and also holds for the
 306 interactions which only occur in the SMEFT, i.e. those proportional to δg and δh , as
 307 well. This also means that the λ and $c_H^{(n)}$ terms are gauge dependent and therefore so is

308 the tadpole. This is also consistent with [7], where they found this dependence exactly
 309 cancels against that of the Higgs two-point function and the loop contributions in the
 310 process $H \rightarrow \gamma\gamma$ at order $\frac{1}{\Lambda^2}$ in the SMEFT, leaving the observable process $H \rightarrow \gamma\gamma$ gauge
 311 invariant as it must be.

312 The sum of the vectors, ghosts, and goldstone bosons, neglecting λ and $c_H^{(n)}$ dependence
 313 is given by:

$$T_H^{V,u,\Phi} = \frac{\bar{M}_W^2}{16\pi^2} \left[(\sqrt{g^{11}})^2 \left\langle \frac{\delta g_{11}}{\delta \hat{h}} \right\rangle - \frac{2}{v} \sqrt{h^{44}} - \left\langle \frac{\delta h_{11}}{\delta \hat{h}} \right\rangle (\sqrt{h^{11}})^2 \right] [2\bar{M}_W^2 - 3A_0(\bar{M}_W)] \\ + \frac{\bar{M}_Z^2}{32\pi^2} \left[\Sigma_{ZZ} - \frac{2}{v} \sqrt{h^{44}} - \left\langle \frac{\delta h_{33}}{\delta \hat{h}} \right\rangle (\sqrt{h^{33}})^2 \right] [2\bar{M}_Z^2 - 3A_0(\bar{M}_Z)]. \quad (72)$$

314 In order to demonstrate the compactness of this expression we expand the quantity in
 315 brackets for the W contribution to $\mathcal{O}(1/\Lambda^4)$ in terms of the Wilson coefficients:

$$\left[(\sqrt{g^{11}})^2 \left\langle \frac{\delta g_{11}}{\delta \hat{h}} \right\rangle - \frac{2}{v} \sqrt{h^{44}} - \left\langle \frac{\delta h_{11}}{\delta \hat{h}} \right\rangle (\sqrt{h^{11}})^2 \right] = -\frac{1}{v} \left[2 + \frac{v^2}{2} \left(c_{H\Box}^{(6)} - c_{HD}^{(6)} + 8c_{HW}^{(6)} \right) \right. \\ \left. + \frac{v^4}{16} \left(12c_{HD}^{(8)} - 20c_{HD,2}^{(8)} + 64c_{HW}^{(8)} + 3(c_{HD}^{(6)} - 4c_{H\Box}^{(6)})^2 + 16(4c_{H\Box}^{(6)} - c_{HD}^{(6)})c_{HW}^{(6)} + 128c_{HW}^{(6)} \right) \right] \\ + \mathcal{O}\left(\frac{1}{\Lambda^6}\right). \quad (73)$$

316

317 In the case of the Z contribution the result depends on many more operator coefficients,
 318 as well as the barred mixing angles due to the dependence in Σ_{ZZ} .

319 The last remaining contribution is from the quantum Higgs boson, which gives:

$$T_H^h = \frac{1}{32\pi^2} (\sqrt{h^{44}})^2 \left[\bar{M}_H^2 \left\langle \frac{\delta h_{44}}{\delta \hat{h}} \right\rangle + v \sqrt{h^{44}} \left(6\lambda - \sum_{n=3}^{\infty} \frac{1}{2^{n-1}} \binom{2n}{1, 2, 2n-3} v^{2n-4} c_H^{(2n)} \right) \right] A_0(\bar{M}_H). \quad (74)$$

320 The sum of all the above contributions to T_H in the SM limit agrees with [7], providing
 321 a useful cross check of the result. To the extent of the authors knowledge the $1/\Lambda^2$ result
 322 does not exist in the literature in the background formalism.

323 With all of the contributions included we can then choose a renormalization condition
 324 related to the tadpole. Returning to Eq. 14 we obtain the coefficient of the tadpole term:

$$t \equiv \frac{\sqrt{h^{44}} v}{16} \left[16\lambda(v_0^2 - v^2) + \sum_{n=1}^{\infty} \frac{(4+2n)v^{4+2n-1}}{2^{2+n}} c_H^{(4+2n)} \right]. \quad (75)$$

325 Choosing $t = 0$ corresponds to the proper ground state [13, 14] and is the scheme we
 326 choose here. At tree level this simply reproduces the condition in Eq. 15. At one loop
 327 this corresponds to cancelling the entire tadpole contribution. Introducing δt as a counter
 328 term, we have the renormalization condition,

$$t = t_0 - \delta t = 0, \quad (76)$$

329 where t_0 corresponds to the tree level contribution. Choosing $t = 0$ corresponds to:

$$\begin{aligned}
\delta t &= -T_H \\
&= + \sum_{\psi} \frac{N_c \bar{M}_{\psi}}{4\pi^2} \left\langle \frac{\delta \mathcal{Y}^{\psi}}{\delta \hat{h}} \right\rangle A_0(\bar{M}_{\psi}) \\
&\quad - \frac{\bar{M}_W^2}{16\pi^2} \left[(\sqrt{g^{11}})^2 \left\langle \frac{\delta g_{11}}{\delta \hat{h}} \right\rangle - \frac{2}{v} \sqrt{h^{44}} - \left\langle \frac{\delta h_{11}}{\delta \hat{h}} \right\rangle (\sqrt{h^{11}})^2 \right] [2\bar{M}_W^2 - 3A_0(\bar{M}_W)] \\
&\quad - \frac{\bar{M}_Z^2}{32\pi^2} \left[\Sigma_{ZZ} - \frac{2}{v} \sqrt{h^{44}} - \left\langle \frac{\delta h_{33}}{\delta \hat{h}} \right\rangle (\sqrt{h^{33}})^2 \right] [2\bar{M}_Z^2 - 3A_0(\bar{M}_Z)] \\
&\quad - \frac{v}{32\pi^2} (\sqrt{h^{11}})^2 \sqrt{h^{44}} \left(4\lambda - \sum_{n=3}^{\infty} \frac{1}{2^{n-3}} \binom{n}{1, 1, n-2} v^{2n-4} c_H^{(2n)} \right) A_0(\sqrt{\xi_W} \bar{M}_W) \\
&\quad - \frac{v}{64\pi^2} (\sqrt{h^{33}})^2 \sqrt{h^{44}} \left(4\lambda - \sum_{n=3}^{\infty} \frac{1}{2^{n-3}} \binom{n}{1, 1, n-2} v^{2n-4} c_H^{(2n)} \right) A_0(\sqrt{\xi_Z} \bar{M}_Z) \\
&\quad - \frac{1}{32\pi^2} (\sqrt{h^{44}})^2 \left[\bar{M}_H^2 \left\langle \frac{\delta h_{44}}{\delta \hat{h}} \right\rangle + v \sqrt{h^{44}} \left(6\lambda - \sum_{n=3}^{\infty} \frac{1}{2^{n-1}} \binom{2n}{1, 2, 2n-3} v^{2n-4} c_H^{(2n)} \right) \right] A_0(\bar{M}_H).
\end{aligned} \tag{77}$$

330 which depends on four barred masses (counting the barred fermion mass only once), four
331 field-space connections plus Σ_{ZZ} , λ , and the sum over $c_H^{(n)}$. Treating the sums as a
332 single entity gives a total dependence on eleven quantities. Conversely, the standard
333 model result depends on four masses and λ . Expanding the tadpole result in terms of
334 the Wilson coefficients of the SMEFT and maintaining barred mass dependence instead
335 gives 12 parameters at dimension six and 21 at $\mathcal{O}(1/\Lambda^4)$ with 9 additional parameters at
336 each subsequent order⁵. In this context the geoSMEFT represents a clear calculational
337 advantage over the traditional approach to the SMEFT.

338 Further, as we saw in the discussion about the gauge, goldstone, and ghost terms, the
339 compactness of the geoSMEFT expressions allows for a straightforward cancellation of
340 terms which would be unclear when expanded in terms of the many Wilson coefficients
341 contributing to each process. Similar simplifications of expressions can be expected for
342 higher n -point functions, and as these expressions will generally be more complicated
343 than those of the tadpole this simplification is crucial to an analytic understanding of the
344 SMEFT expansion at one loop.

345 6 Conclusions

346 We have constructed the Feynman rules necessary for the calculation of the tadpole di-
347 agram within the framework of the geoSMEFT. In doing so we have included, for the
348 first time, the gauge fixing of the geoSMEFT and the all-orders Feynman rules related to
349 gauge fixing which include a single background Higgs boson and two other particles. We
350 proceeded to calculate all diagrams contributing to the process. The results allowed us
351 to fix the minimum of the Higgs potential at one loop and to all orders in the SMEFT
352 power counting. In doing so we demonstrated the simplicity of expressions obtained in the
353 geoSMEFT as compared with those expanded in terms of the Wilson coefficients which is
354 necessary in standard approaches to the SMEFT. Further we obtained not only the first
355 one-loop calculation including full next to leading order results in the SMEFT, but the

⁵The number of new parameters in h_{IJ} , g_{AB} , and \mathcal{Y} at a given dimension above six stays constant, see Table 1 of [10].

356 first one-loop calculation including all orders contributions in $1/\Lambda^n$. As discussed in the
357 introduction and Appendix B, the tadpole diagram is not only essential to fully defining
358 one-loop results, such as the masses of the gauge bosons, but is also essential for the gauge
359 invariance of the theory at one loop. This demonstrates the foundational nature of this
360 work toward future precision calculations in the geoSMEFT.

361 Beyond the scope of the calculations contained in this article, we note that the geo-
362 SMEFT is currently defined to include vertices of up to any three particles accompanied
363 by arbitrarily many scalar field insertions. This has presented the opportunity for many
364 all-orders results at tree level [6, 11] and their projection to order $1/\Lambda^4$ in phenom-
365 logical studies. This allows for the possibility to perform a truncation error analysis
366 more consistent with the SMEFT than those commonly used where partial dimension-six
367 squared results are used to estimate the truncation error. While few additional one-loop
368 calculations are currently possible in the framework of the geoSMEFT, it is possible to
369 systematically extend the geoSMEFT to include any N particles plus arbitrarily many
370 scalar field insertions. In particular, the expansion in the vacuum expectation value can
371 be defined for arbitrary n -point functions by simply defining the field-space connections
372 for ever increasing numbers of fields, i.e. for increased numbers of variations in Eq. 2. The
373 derivative expansion is more difficult as, beyond three points functions, arbitrary powers
374 of the momenta can be included leading to an infinite number of operators contributing
375 to any given n -point function [10]. Nonetheless, the derivative expansion can separately
376 be truncated at a given order. This will allow for the all orders in $(v/\Lambda)^n$, as well as
377 $(p/\Lambda)^n$ to a truncated order, calculation of all two-point functions in the near future and
378 subsequently higher n -point functions. With all orders results at tree- and one-loop level
379 we can then define a fully consistent truncation error associated with the SMEFT. This
380 is an important step toward a precision program for the studies at the High Luminosity
381 LHC as well as for supporting and informing the case for next generation colliders.

382

383 Acknowledgements

384 TC thanks M. Trott, A. Martin, and J. Talbert for useful discussions and their reading of
385 the manuscript.

386 **Funding information** TC acknowledges funding from European Union's Horizon 2020
387 research and innovation program under the Marie Skłodowska-Curie grant agreement No.
388 890787.

389 A Useful geoSMEFT definitions and relations

390 The following definitions and geometric relations are used extensively throughout this
 391 work in order to simplify expressions and retain them in the geometric formulation. These
 392 relations can be found in [10]. The following matrices are used to define the covariant
 393 derivatives, field strength tensors, and field-space connections:

$$\gamma_{1,J}^I = \begin{bmatrix} 0 & 0 & 0 & -1 \\ 0 & 0 & -1 & 0 \\ 0 & 1 & 0 & 0 \\ 1 & 0 & 0 & 0 \end{bmatrix}, \quad \gamma_{2,J}^I = \begin{bmatrix} 0 & 0 & 1 & 0 \\ 0 & 0 & 0 & -1 \\ -1 & 0 & 0 & 0 \\ 0 & -1 & 0 & 0 \end{bmatrix}, \quad (78)$$

394

$$\gamma_{3,J}^I = \begin{bmatrix} 0 & -1 & 0 & 0 \\ 1 & 0 & 0 & 0 \\ 0 & 0 & 0 & -1 \\ 0 & 0 & 1 & 0 \end{bmatrix}, \quad \gamma_{4,J}^I = \begin{bmatrix} 0 & -1 & 0 & 0 \\ 1 & 0 & 0 & 0 \\ 0 & 0 & 0 & 1 \\ 0 & 0 & -1 & 0 \end{bmatrix}, \quad (79)$$

395 as well as:

$$\Gamma_{1,J}^I = \begin{bmatrix} 0 & 0 & 1 & 0 \\ 0 & 0 & 0 & -1 \\ 1 & 0 & 0 & 0 \\ 0 & -1 & 0 & 0 \end{bmatrix}, \quad \Gamma_{2,J}^I = \begin{bmatrix} 0 & 0 & 0 & 1 \\ 0 & 0 & 1 & 0 \\ 0 & 1 & 0 & 0 \\ 1 & 0 & 0 & 0 \end{bmatrix}, \quad (80)$$

396

$$\Gamma_{3,J}^I = \begin{bmatrix} -1 & 0 & 0 & 0 \\ 0 & -1 & 0 & 0 \\ 0 & 0 & 1 & 0 \\ 0 & 0 & 0 & 1 \end{bmatrix}, \quad \Gamma_{4,J}^I = \begin{bmatrix} -1 & 0 & 0 & 0 \\ 0 & -1 & 0 & 0 \\ 0 & 0 & -1 & 0 \\ 0 & 0 & 0 & -1 \end{bmatrix}. \quad (81)$$

397 The quantities with tildes are defined as:

$$\begin{aligned} \tilde{\epsilon}^A{}_{BC} &= g_2 \epsilon^A{}_{BC} && \text{with } \tilde{\epsilon}^1{}_{23} = g_2 \quad \text{and } \tilde{\epsilon}^4{}_{BC} = 0, \\ \tilde{\gamma}_{A,J}^I &= \begin{cases} g_2 \gamma_{A,J}^I, & \text{for } A = 1, 2, 3, \\ g_1 \gamma_{A,J}^I, & \text{for } A = 4. \end{cases} \end{aligned} \quad (82)$$

398 The relation between barred and unbarred couplings is:

$$\bar{g}_2 = g_2 \sqrt{g}^{11} = g_2 \sqrt{g}^{22}, \quad (83)$$

$$\bar{g}_Z = \frac{g_2}{c_{\theta_Z}^2} (\bar{c}_W \sqrt{g}^{33} - \bar{s}_W \sqrt{g}^{34}) = \frac{g_1}{s_{\theta_Z}^2} (\bar{s}_W \sqrt{g}^{44} - \bar{c}_W \sqrt{g}^{34}), \quad (84)$$

$$\bar{e} = g_1 (\bar{s}_W \sqrt{g}^{33} + \bar{c}_W \sqrt{g}^{34}) = g_1 (\bar{c}_W \sqrt{g}^{44} + \bar{s}_W \sqrt{g}^{34}). \quad (85)$$

399 The above expressions make use of the barred mixing angles:

$$s_{\theta_Z}^2 = \frac{g_1(\sqrt{g}^{44} \bar{s}_W - \sqrt{g}^{34} \bar{c}_W)}{g_2(\sqrt{g}^{33} \bar{c}_W - \sqrt{g}^{34} \bar{s}_W) + g_1(\sqrt{g}^{44} \bar{s}_W - \sqrt{g}^{34} \bar{c}_W)}, \quad (86)$$

$$\bar{s}_W^2 = \frac{(g_1 \sqrt{g}^{44} - g_2 \sqrt{g}^{34})^2}{g_1^2[(\sqrt{g}^{34})^2 + (\sqrt{g}^{44})^2] + g_2^2[(\sqrt{g}^{33})^2 + (\sqrt{g}^{34})^2] - 2g_1 g_2 \sqrt{g}^{34}(\sqrt{g}^{33} + \sqrt{g}^{44})} \quad (87)$$

400 The barred masses are given by:

$$\bar{M}_W^2 = \frac{\bar{g}_2^2}{4} \sqrt{h_{11}}^{-2} v^2, \quad (88)$$

$$\bar{M}_Z^2 = \frac{\bar{g}_Z^2}{4} \sqrt{h_{33}}^{-2} v^2, \quad (89)$$

$$\bar{M}_A^2 = 0. \quad (90)$$

401 Expanding the elements of the field-space connections of Eqs. 5, 6, and 16–18 become
 402 complicated very quickly, supporting the use of the geometric approach. Some examples
 403 of elements of the matrices include:

$$\sqrt{g}^{11} = 1 + c_{HW}^{(6)} v^2 + \frac{1}{2} [c_{HW}^{(8)} + 3(c_{HW}^{(6)})^2] v^4 \quad (91)$$

$$\sqrt{h}^{44} = 1 + \frac{1}{4} [4c_{H\Box}^{(6)} - c_{HD}^{(6)}] v^2 + \frac{1}{32} [3(c_{HD}^{(6)} - c_{H\Box}^{(6)})^2 - 4c_{HD}^{(8)} - 4c_{HD,2}^{(8)}] v^4 + \mathcal{O}\left(\frac{1}{\Lambda^6}\right) \quad (92)$$

404

405 B Relevance of the tadpole to renormalization

406 Here we outline the importance of the tadpole to renormalization. We proceed by outline
 407 the renormalization procedure to arrive at the implications of the tadpole diagram in the
 408 FJ tadpole scheme, we do not employ the BFM here for simplicity. We loosely follow the
 409 notation of [15]. The fields are renormalized as follows:

$$h_0 = \sqrt{Z_{\hat{h}}} h_R \quad (93)$$

$$W_0^\pm = \sqrt{Z_W} W_R^\pm \quad (94)$$

$$(95)$$

410 The fourth component of the real scalar field is renormalized as:

$$\phi_4 = v_0 + \hat{h}_0 \rightarrow Z_v v_R + \delta v + \sqrt{Z_h} h_R \quad (96)$$

411 Expanding the scalar potential of Eq. 14 about the tree level vacuum expectation value
 412 and adding the one-loop tadpole contribution we find:

$$t = -2\lambda_R v_R \delta v + T_H \equiv \delta t + T_H \quad (97)$$

413 This defines the relationship between δt and δv , in the main text δt is chosen such that
 414 $t = 0$. This is equivalent to the choice:

$$\delta v = \frac{1}{2\lambda_R v_R^2} T_H = \frac{1}{M_{H,R}^2} T_H \quad (98)$$

415 Employing an on-shell renormalization scheme as in [15] the one loop shifts in masses
 416 of the vector bosons ($V = W, Z$) are given by:

$$\frac{\bar{m}_{V,R}^2}{\bar{m}_V^2} = 1 + 2\frac{\delta v}{v} - \frac{\delta m_V^2}{m_V^2}, \quad (99)$$

417 where δv corresponds to the correction outlined above, and δm_V^2 corresponds to the explicit
 418 contribution from the transverse part of the one-loop two-point functions:

$$\delta m_V^2 = \text{Re}[\Sigma_T^{VV}(M_p^2)]. \quad (100)$$

419 In this way we can see from Eq. 99 that even in the FJ tadpole scheme employed in
 420 this article, the one-loop tadpole is still phenomenologically relevant as it shifts the masses
 421 of the gauge bosons. Further, as the tadpole was found to be gauge-parameter dependent
 422 in Sec 5, we see that the gauge-independence of results such as the shifted masses depend
 423 on the tadpole diagram. In this way we have demonstrated the importance of the tadpole
 424 diagram to the future one-loop geSMEFT program both phenomenologically and in terms
 425 of gauge invariance of the theory, which is necessary for the consistency of the QFT.

References

- 426
- 427 [1] C. Hays, A. Martin, V. Sanz and J. Setford, *On the impact of dimension-*
428 *eight SMEFT operators on Higgs measurements*, JHEP **02**, 123 (2019),
429 doi:10.1007/JHEP02(2019)123, 1808.00442.
- 430 [2] L. Lehman and A. Martin, *Hilbert Series for Constructing Lagrangians: ex-*
431 *anding the phenomenologist's toolbox*, Phys. Rev. D **91**, 105014 (2015),
432 doi:10.1103/PhysRevD.91.105014, 1503.07537.
- 433 [3] L. Lehman and A. Martin, *Low-derivative operators of the Standard Model*
434 *effective field theory via Hilbert series methods*, JHEP **02**, 081 (2016),
435 doi:10.1007/JHEP02(2016)081, 1510.00372.
- 436 [4] B. Henning, X. Lu, T. Melia and H. Murayama, *2, 84, 30, 993, 560, 15456, 11962,*
437 *261485, ...: Higher dimension operators in the SM EFT*, JHEP **08**, 016 (2017),
438 doi:10.1007/JHEP08(2017)016, [Erratum: JHEP 09, 019 (2019)], 1512.03433.
- 439 [5] R. Boughezal, E. Mereghetti and F. Petriello, *Dilepton production in the SMEFT at*
440 $\mathcal{O}(1/\Lambda^4)$ (2021), 2106.05337.
- 441 [6] T. Corbett, A. Helset, A. Martin and M. Trott, *EWPD in the SMEFT to dimension*
442 *eight* (2021), 2102.02819.
- 443 [7] C. Hartmann and M. Trott, *On one-loop corrections in the standard model*
444 *effective field theory; the $\Gamma(h \rightarrow \gamma\gamma)$ case*, JHEP **07**, 151 (2015),
445 doi:10.1007/JHEP07(2015)151, 1505.02646.
- 446 [8] C. Hartmann and M. Trott, *Higgs Decay to Two Photons at One Loop in the*
447 *Standard Model Effective Field Theory*, Phys. Rev. Lett. **115**(19), 191801 (2015),
448 doi:10.1103/PhysRevLett.115.191801, 1507.03568.
- 449 [9] A. Helset, M. Paraskevas and M. Trott, *Gauge fixing the Standard*
450 *Model Effective Field Theory*, Phys. Rev. Lett. **120**(25), 251801 (2018),
451 doi:10.1103/PhysRevLett.120.251801, 1803.08001.
- 452 [10] A. Helset, A. Martin and M. Trott, *The Geometric Standard Model Effective Field*
453 *Theory*, JHEP **03**, 163 (2020), doi:10.1007/JHEP03(2020)163, 2001.01453.
- 454 [11] C. Hays, A. Helset, A. Martin and M. Trott, *Exact SMEFT formulation and expansion*
455 *to $\mathcal{O}(v^4/\Lambda^4)$* , JHEP **11**, 087 (2020), doi:10.1007/JHEP11(2020)087, 2007.00565.
- 456 [12] T. Corbett, *The Feynman rules for the SMEFT in the background field gauge*, JHEP
457 **03**, 001 (2021), doi:10.1007/JHEP03(2021)001, 2010.15852.
- 458 [13] J. Fleischer and F. Jegerlehner, *Radiative Corrections to Higgs Decays*
459 *in the Extended Weinberg-Salam Model*, Phys. Rev. D **23**, 2001 (1981),
460 doi:10.1103/PhysRevD.23.2001.
- 461 [14] A. Denner, G. Weiglein and S. Dittmaier, *Application of the background field method*
462 *to the electroweak standard model*, Nucl. Phys. B **440**, 95 (1995), doi:10.1016/0550-
463 3213(95)00037-S, hep-ph/9410338.
- 464 [15] T. Corbett, A. Martin and M. Trott, *Consistent higher order $\sigma(\mathcal{G}\mathcal{G} \rightarrow h)$, $\Gamma(h \rightarrow \mathcal{G}\mathcal{G})$*
465 *and $\Gamma(h \rightarrow \gamma\gamma)$ in geoSMEFT* (2021), 2107.07470.

- 466 [16] T. Corbett and M. Trott, *One loop verification of SMEFT Ward Identities* (2020),
467 2010.08451.
- 468 [17] T. Corbett, A. Helset and M. Trott, *Ward Identities for the Stan-*
469 *dard Model Effective Field Theory*, Phys. Rev. D **101**(1), 013005 (2020),
470 doi:10.1103/PhysRevD.101.013005, 1909.08470.
- 471 [18] W. Dekens and P. Stoffer, *Low-energy effective field theory below the electroweak*
472 *scale: matching at one loop*, JHEP **10**, 197 (2019), doi:10.1007/JHEP10(2019)197,
473 1908.05295.
- 474 [19] G. Buchalla, A. Celis, C. Krause and J.-N. Toelstede, *Master Formula for One-Loop*
475 *Renormalization of Bosonic SMEFT Operators* (2019), 1904.07840.